Imperial College London

COURSEWORK

PRINCIPLES OF CLASSICAL AND MODERN RADAR

DEPARTMENT OF ELECTRICAL AND ELECTRONIC ENGINEERING

Monostatic Pulse Radar for Complex Targets

Student name:
Leonidas Tsigkounakis
CID: 01927913

Professor:
Athanasios Manikas

GTAs:
Yunhao Liu

Contents

1 Introduction

A PC-based monostatic pulse radar system is simulated with MATLAB whose architecture employs a uniform linear phased array of 45 isotropic antennas for both the transmitter and the receiver (`generate_ULA.m`). This allows electronic steering of the net radiation to a desired azimuth angle θ without any mechanical motion. The MATLAB simulations also include the baseband signal generator for the coded pulse (`generate_pulse_train.m`), the Tx & Rx phase shifters in complex exponential form (`psi_steer.m`), the channel modelling function which generates the backscatter data used in tasks 3-6 (`generate_backscatter.m`) and the transmitter (`Tx_prep.m`) and receiver (`Rx_prep.m`) modules which transform the 1×11200 signals into 45×11200 matrices and vice-versa. For the signal processing module (after point Z) the simulation involves a matched filter to maximise the SNR (`generate_MF.m`), a non-coherent PRI integrator (`generate_noncoherent_PRI_integration.m`) and finally a function that yields the voltage threshold for target detection according to the Newman-Pearson criterion (`generate_threshold.m`). The radar operates in the middle of the Ku frequency band. This implies that the carrier has a frequency of 15GHz and a wavelength of 0.02m in free space. The coded pulse that is transmitted has a duration $T_p = 196ns$ and is repeated every $T_{PRI} = 200T_P = 39.2\mu s$. The pulse is modulated with the code sequence [-1, -1, -1, +1, +1, -1, -1] which increases bandwidth and the range resolution. Specifically, the range resolution is given by $\triangle R = \frac{1}{2}c\frac{T_p}{7} = 4.2m$. This means that the system cannot distinguish between objects/features that are less than 4.2m apart. Another limitation imposed on the range parameter is related to range ambiguities. A return from prior pulses would imply that the target's true position is much further away than estimated. Therefore a targets range must not be grater than $R_{max} = \frac{1}{2}cT_{PRI} = 5880m$. The radar operates in the x-y plane with azimuth angle $\theta \in [30°, 150°]$. The main lobe created by the phased array spends 8 pulse repetition intervals per $1°$ in that range. Therefore the dwell time is $T_{dwell} = 8T_{PRI} = 313.6\mu s$, and, finally, the total scan/sweep time is $T_{scan} = 121T_{dwell} = 3.795ms$.

2 Tasks

2.1 Phase shifters

Phase shifters allow steering of the main lobe of the antenna array to a predetermined direction. Since there are a total of 45 isotropic antennas in use, the maximum gain at a specific steering direction is 45. Under the MATLAB file `Task_1.m`, the `theta_main` parameter on line 15 determines the steering angle that is used to calculate the steering angle vectors called `angles_Tx` and `angles_Rx`. Figure 1 illustrates the antenna array patterns in polar form for $40°$, $70°$ and $120°$.

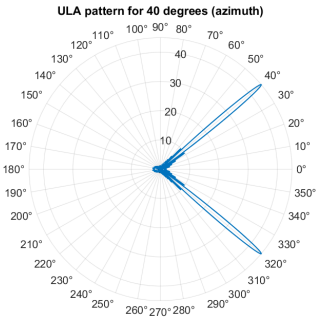

(a) $40°$.

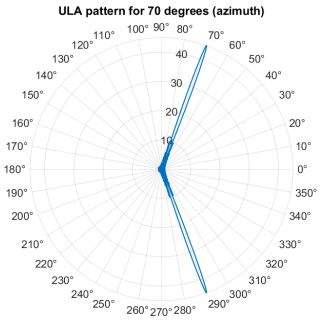

(b) $70°$.

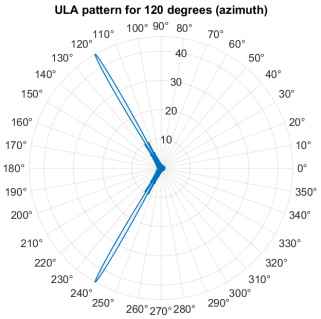

(c) $120°$.

Figure 1: Uniform linear array pattern for specific directions - Polar plots.

The linear representation of each antenna array pattern is shown in figure 8 of the appendix. Also, within the submitted .zip file, the folder called "Misc" under "Images for report" has a GIF file that animates the steered lobe from 0 to 180 degrees. It is observed that the lobe is narrowest at $90°$ and that it's shape is significantly altered at low angles due to interference from the mirrored counterpart. This explains the 30-150 degree limitation of the radar system.

2.2 Matlab backscatter modelling function

The channel between transmitter and receiver can be modelled as a linear filter with impulse response h[n]. This implies that the Tx signal can be convolved with the channel's impulse response to yield the signal at the receiver's end. After the coded pulse train has been generated and has been prepared for transmission, the `generate_backscatter.m` function is then used to generate artificial backscatter data. This function needs to take into consideration the target parameters (if any), the additive noise and it also has to perform the previously mentioned convolution:

$$s[n] = AWGN[n] + \sum_{\ell=1}^{M} \sqrt{\frac{G_{Tx}G_{Rx}}{(4\pi)^3} RCS \frac{\lambda_c}{R^2}} \exp\left(-j2\pi f_c \frac{2R}{c}\right) \exp\left(j\psi\right) S_{Rx,l} S_{Tx,l}{}^H x[n - n_{echo,l}]$$

2.3 1st scan - no targets

For the first scan it is assumed that there are no targets present. This will result in signals at the baseband ports with only noise. Antenna 28 is arbitrarily chosen for the noise magnitude plot snapshot for one dwell-time. Moreover, again for antenna 28, the estimated Rayleigh pdf of the noise samples along with their histogram are shown on figure 2:

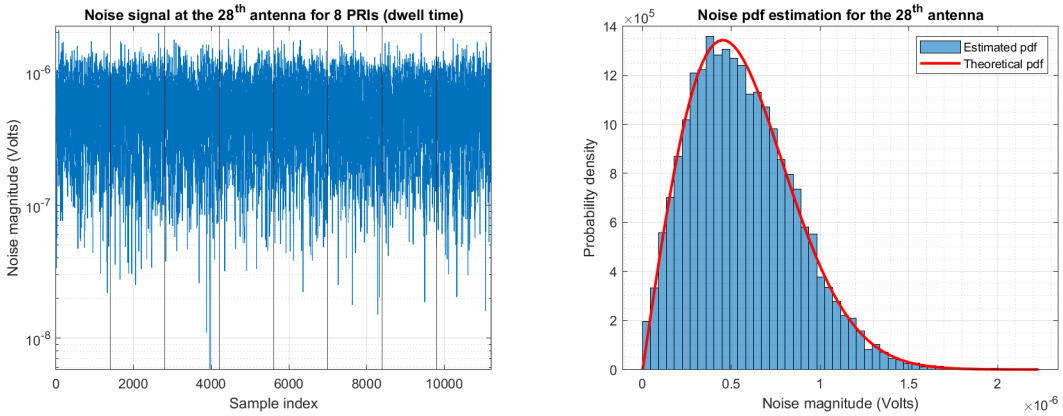

(a) Noise magnitude vs sample index. **(b)** Noise magnitude histogram and pdf.

Figure 2: Noise signal and statistics for the 28^{th} antenna for one dwell-time

The signal at point Z has dimensions 1×11200 and is also purely noise. In figures 9 and 10 of the appendix the magnitude snapshot and the relevant histogram of the noise at point Z can be also found. To calculate the average complex power of a complex signal one can use $P_z = \frac{1}{M}\sum_{n=1}^{M} z[n] * z[n]^*$. In order to obtain the real power (and not the reactive power) it is necessary to take the real part of the above quantity. Performing the above calculation yields an average power at point Z of $1.839 \times 10^{-11} W$. Since this is the only part of the coursework where there is only noise in the Rx signal at point Z, the detection threshold voltage is also calculated using `generate_threshold.m` with a probability of false alarm of 10^{-3}. The voltage threshold found is approximately $8.7 \times 10^{-6} V$ and is stored as a separate MATLAB data file for use in the next tasks.

2.4 2nd scan - one target

First, it is assumed that the target parameters are known and thus the backscatter function from task 2 can be used to generate the signal at point Z as illustrated under figure 3.

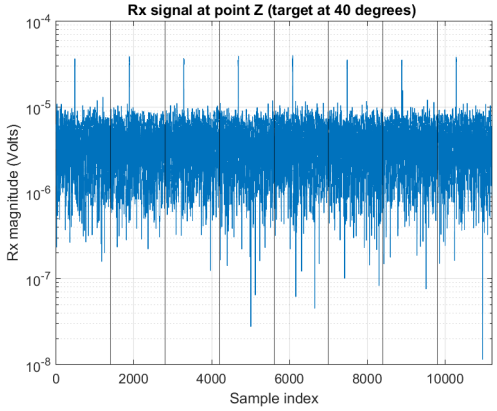

Figure 3: Backscatter data at point Z for target located at 40 degrees

Given the simulated data at point Z the aim is to reverse engineer the process and estimate the target's parameters. Initially, an angle sweep is necessary to observe the strength of the received

signal and to then estimate the target's azimuth angle. The plot for the angle sweep is in figure 11 of the appendix. The peak occurs at 40 degrees which is indeed the true angle of the object. Now that the angle is found, the data at point Z corresponding to a steer of 40 degrees can be used. The signal is passed through a matched filter for SNR maximisation (figure 12) and then from a non-coherent PRI integrator (figure 13) so that the signal spans only one PRI. Then, given that the peak exceeds the voltage threshold calculated in task 3, the echo time and range can be calculated from the peak's sample index. The next step involves the RCS estimation. The radar equation can be solved with respect to the RCS since all parameters are known. The estimated values for the target at $40°$ are shown on table 1 below.

	Target Estimated Parameters
θ	$40°$
Range	$2003.4m$
Avg. RCS	$1.0528m^2$

Table 1: Estimated parameters for target 1.

The estimated target parameters are indeed similar to the true values. To calculate the average RCS, an average of 10 measurements were taken.

2.5 3^{rd} scan - two targets

During the second scan there are two targets present whose parameters are given in the specification sheet. In a similar way to the previous task the simulated backscatter data at point Z is shown in figure 4 for the two targets. The angle sweep (figure 14) reveals the presence of the two

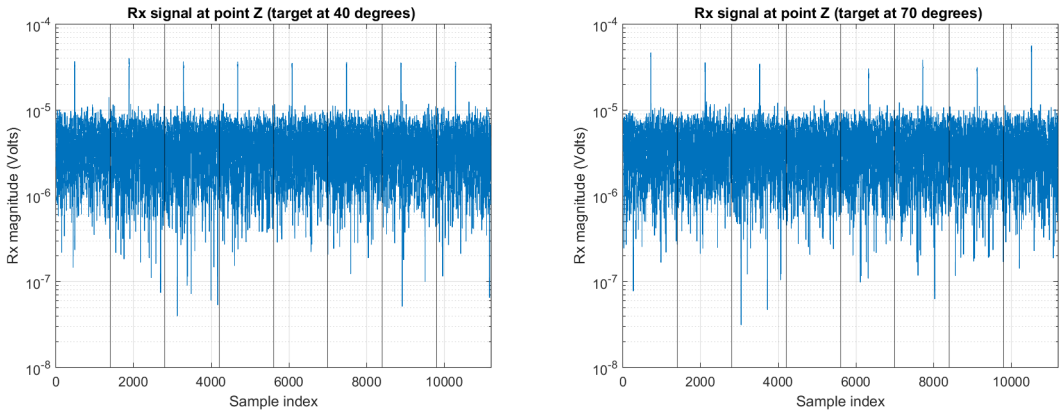

(a) Target at $40°$.

(b) Target at $70°$.

Figure 4: Simulated backscatter data at point Z.

targets at their respective angles. The matched filter's and non-coherent PRI integrator's output can be also seen, respectively, in figures 15 and 16 of the appendix. Finally, the estimated target parameters are shown below on table 2.

	Target Estimated Parameters
θ	$40° \mid 70°$
Range	$2003.4m \mid 3003m$
Avg. RCS	$1.0528m^2 \mid 5.1414m^2$

Table 2: Estimated parameters for targets 1 and 2.

The target at $70°$ does not have a dominant scatterer (class-1 scatterer). Indeed the target's estimated RCS varied significantly in each run. 20 measurements were averaged out to obtain the average RCS value for the second target.

2.6 4^{th} scan - three targets

A third target has now been added at $120°$. The simulated backscatter signals for each target at point Z are shown below in figure 5. The angle sweep plot accurately reveals the direction

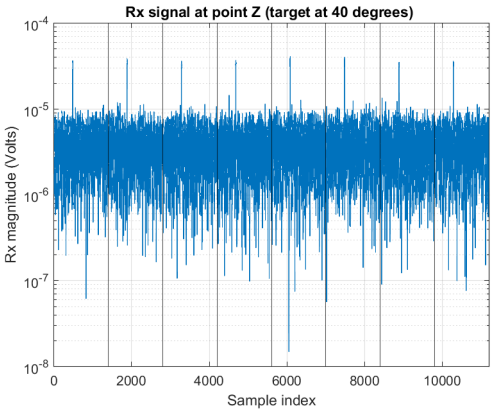

(a) Target at $40°$.

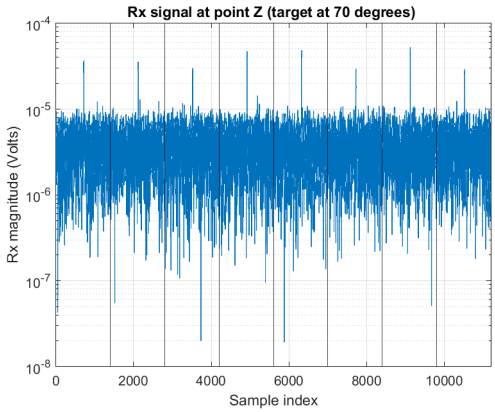

(b) Target at $70°$.

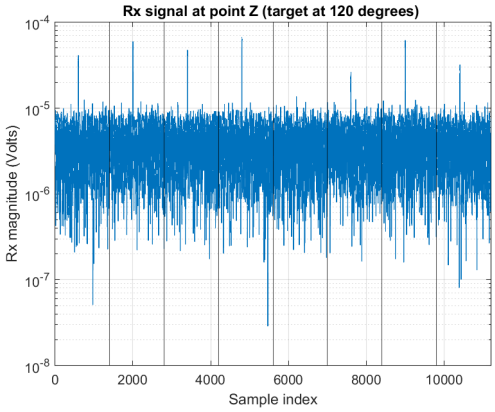

(c) Target at $120°$.

Figure 5: Simulated backscatter data at point Z.

of the three targets as can be observed in figure 17. The matched filter's and non-coherent PRI integrator's output for each of the three targets is illustrated in figures 18 and 19. Finally, table 3 shows the estimated parameters for all three targets. Target 3 has a dominant scatter (class 2

	Target Estimated Parameters
θ	$40°$ | $70°$ | $120°$
Range	$2003.4m$ | $3003m$ | $2503.2m$
Avg. RCS	$1.0528m^2$ | $5.1414m^2$ | $4.6391m^2$

Table 3: Estimated parameters for targets 1, 2 and 3.

scatterer). Indeed the RCS estimate was less volatile than that of target 2. 10 values were averaged to obtained the average RCS for target 3.

2.7 Radar data - multi-target detection and parameter estimation

In this task backscatter data is provided without the knowledge of target parameters before-hand. A similar approach to the reverse engineering of the target parameters will be applied. First an angle sweep is done to determine the presence of targets as shown on figure 6.

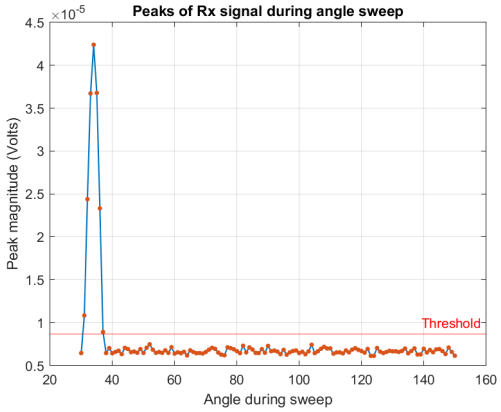

Figure 6: Maximum of backscatter data at point Z from $30°$ to $150°$ with a step of $1°$.

It is evident that there is at least one target located at $34°$. The next step is to pass the signal at point Z through the matched filter and then through the non-coherent PRI integrator. The resulting signals are shown in figures 7a and 7b respectively.

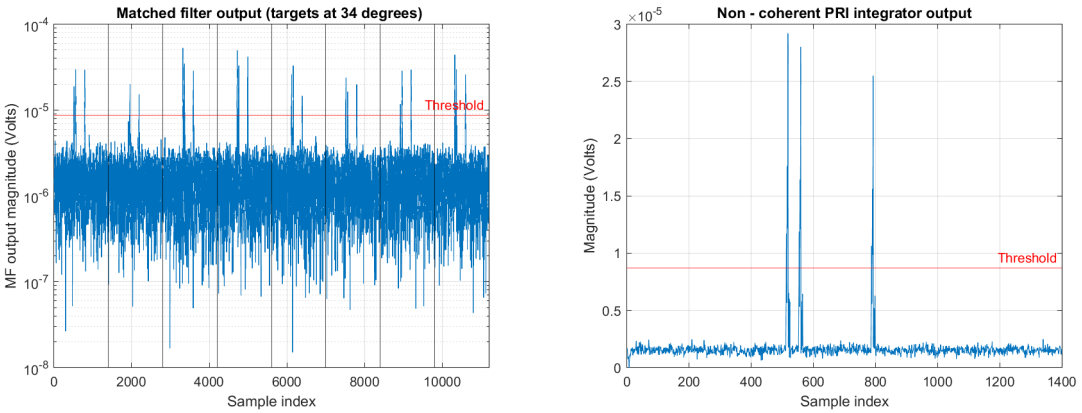

(a) Signals at matched filter's output.

(b) Signals at non-coherent PRI integrator's output.

Figure 7: Matched filter and non-coherent PRI integrator outputs for backscatter data.

It can be observed that there are three targets present. Similarly to the previous tasks, their parameters are estimated. The values obtained are shown in table 4.

	Target Estimated Parameters
θ	$34°$ | $34°$ | $34°$
t_{echo}	$14.308\mu s$ | $15.456\mu s$ | $21.98\mu s$
Range	$2146.2m$ | $2318.4m$ | $3297m$
Avg. RCS	$2.0493m^2$ | $2.7905m^2$ | $11.4131m^2$

Table 4: Estimated parameters for the three targets detected.

3 Appendix

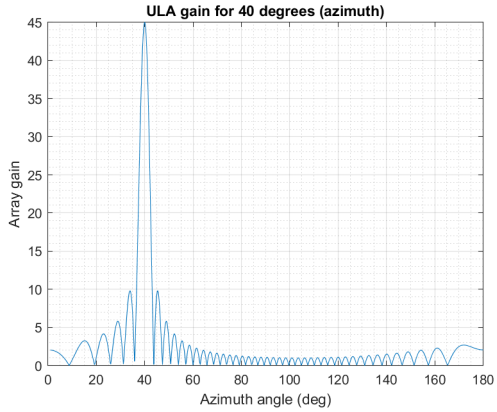

(a) $40°$.

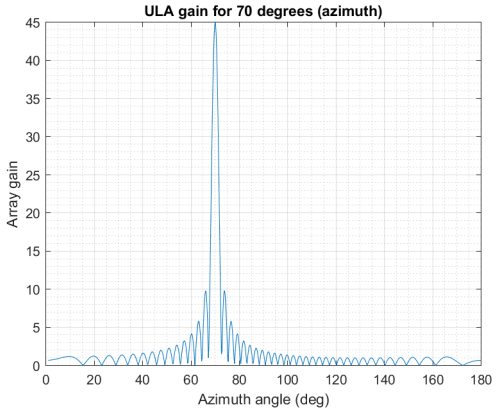

(b) $70°$.

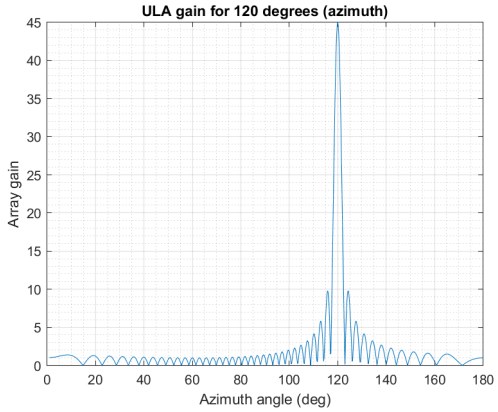

(c) $120°$.

Figure 8: Uniform linear array pattern for specific directions - Linear plots.

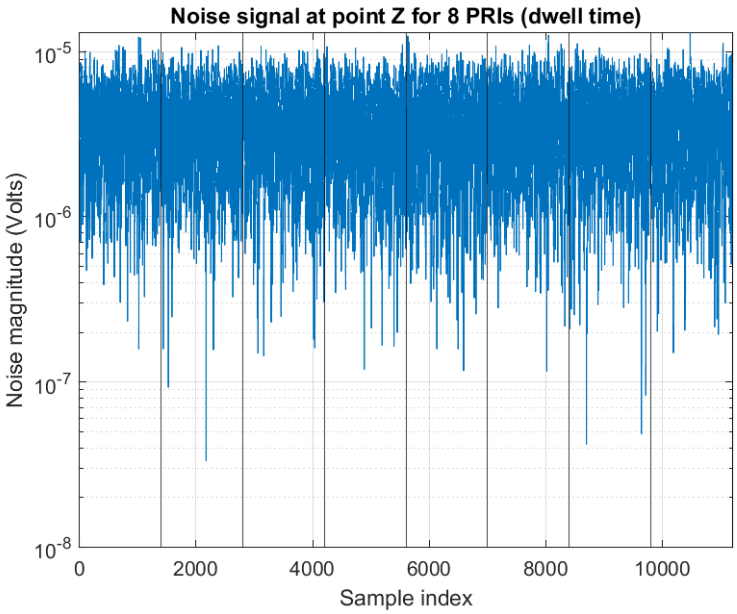

Figure 9: Noise magnitude vs sample index at point Z.

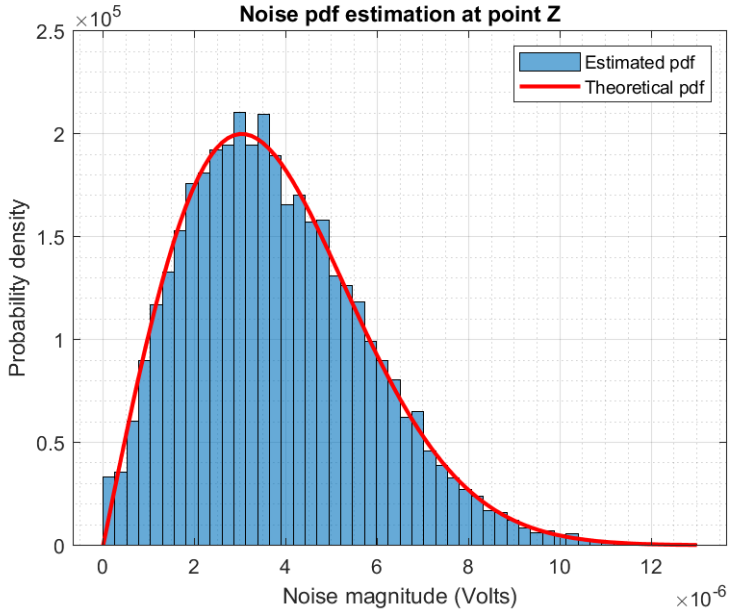

Figure 10: Noise magnitude histogram and theoretical pdf at point Z.

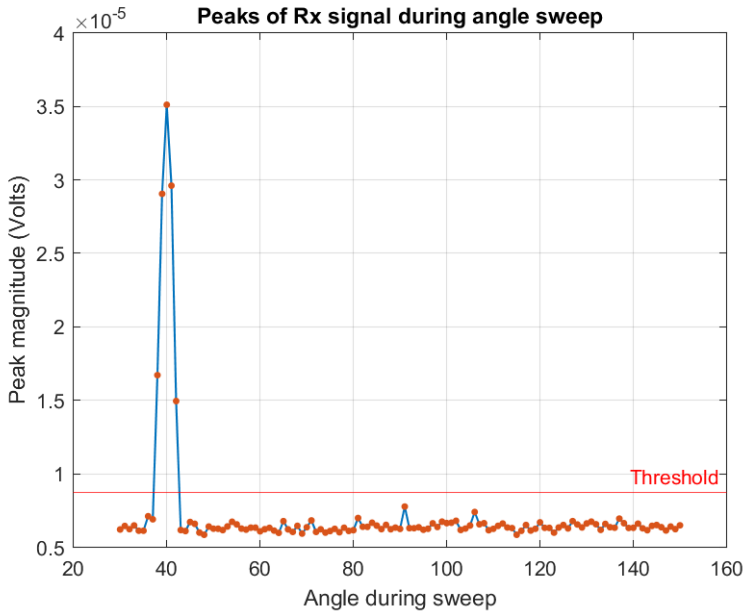

Figure 11: Maximum of backscatter data at point Z from $30°$ to $150°$ with a step of $1°$.

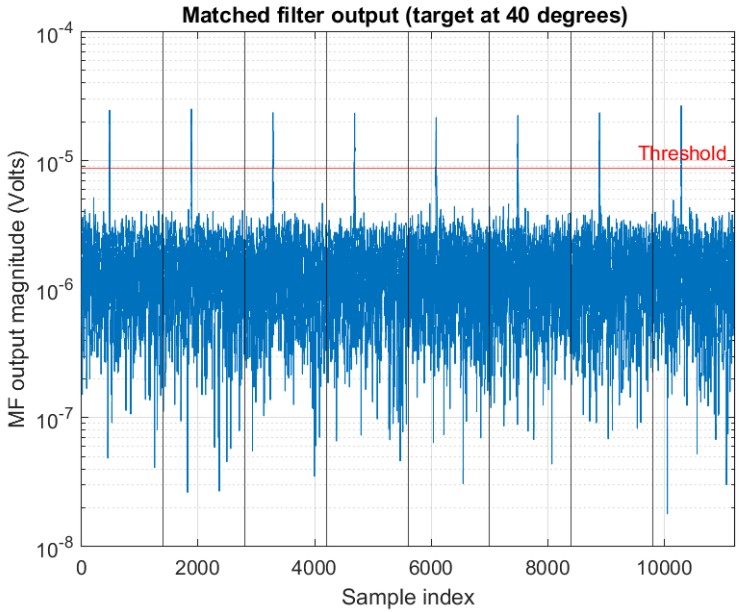

Figure 12: Signals at matched filter's output.

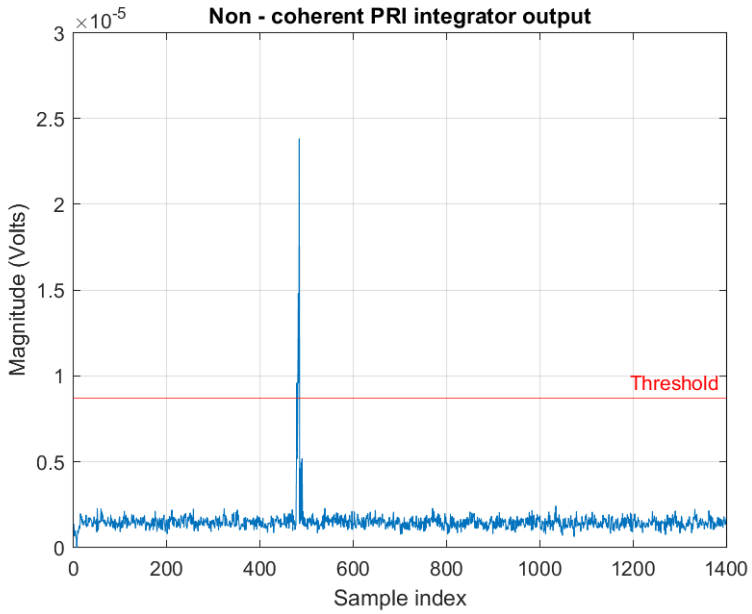

Figure 13: Signals at non-coherent PRI integrator's output.

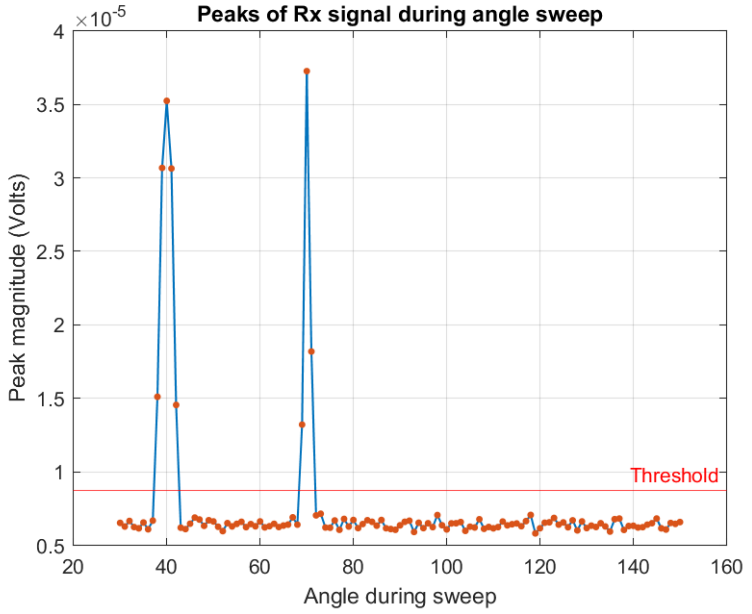

Figure 14: Maximum of backscatter data at point Z from $30°$ to $150°$ with a step of $1°$.

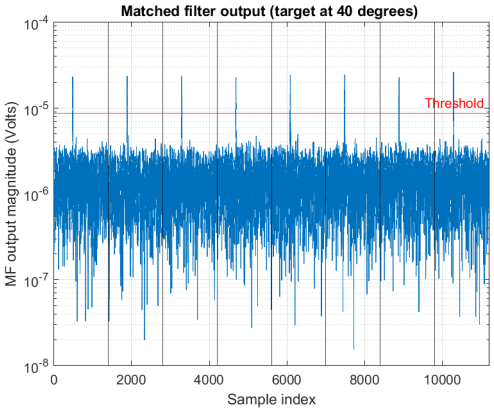

(a) Target at $40°$.

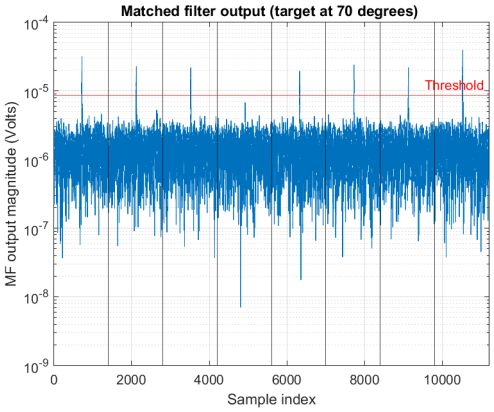

(b) Target at $70°$.

Figure 15: Signals at matched filter's output.

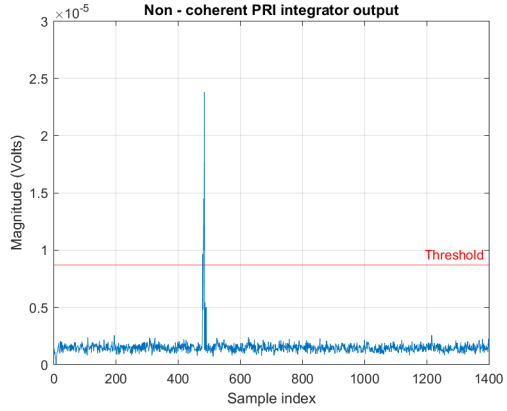

(a) Target at $40°$.

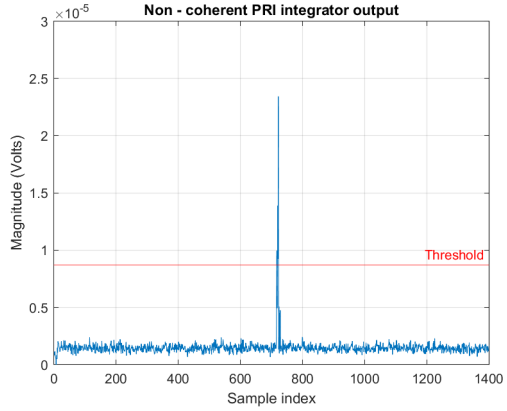

(b) Target at $70°$.

Figure 16: Signals at non-coherent PRI integrator's output.

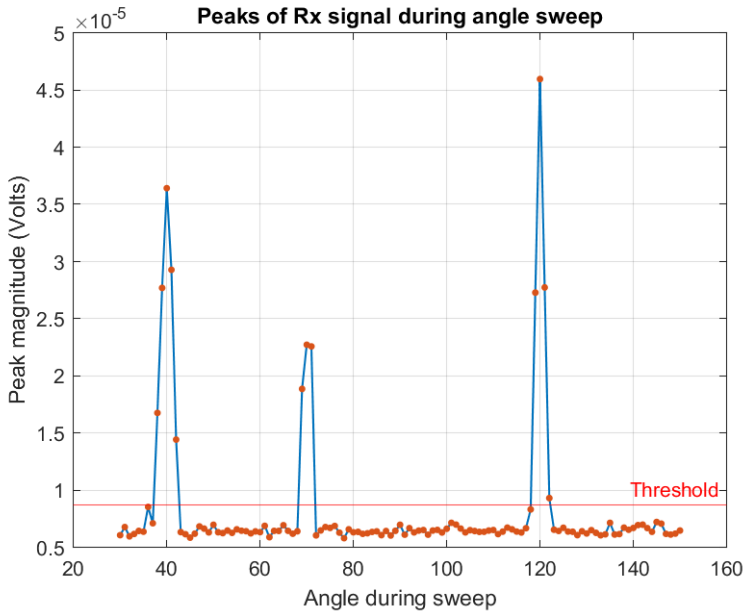

Figure 17: Maximum of backscatter data at point Z from $30°$ to $150°$ with a step of $1°$.

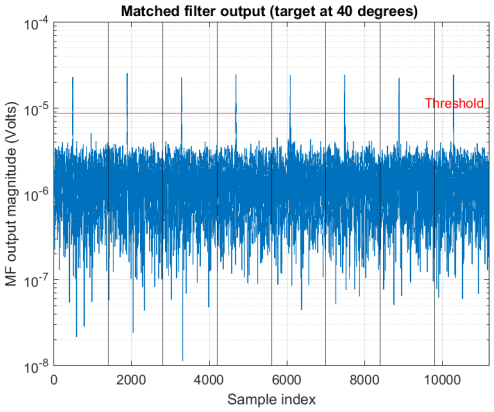

(a) Target at $40°$.

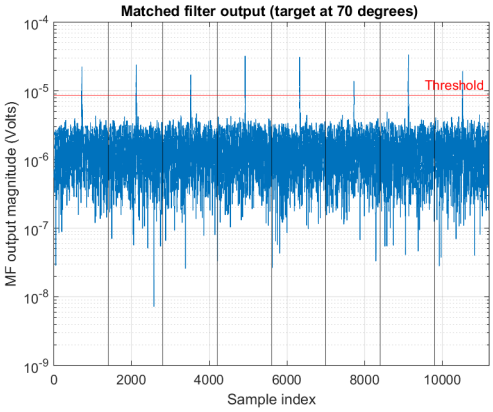

(b) Target at $70°$.

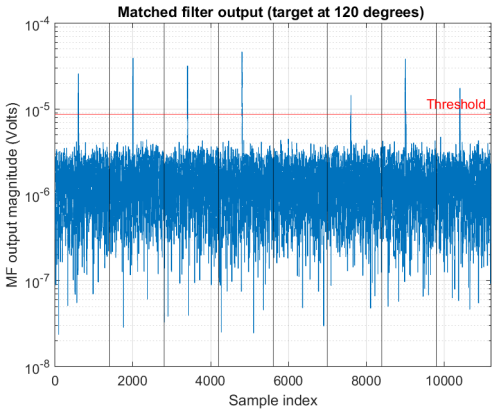

(c) Target at $120°$.

Figure 18: Signals at matched filter's output.

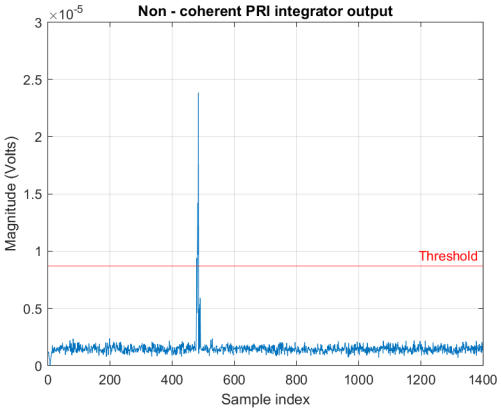

(a) Target at $40°$.

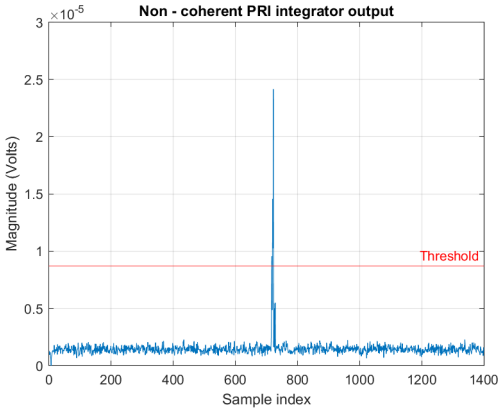

(b) Target at $70°$.

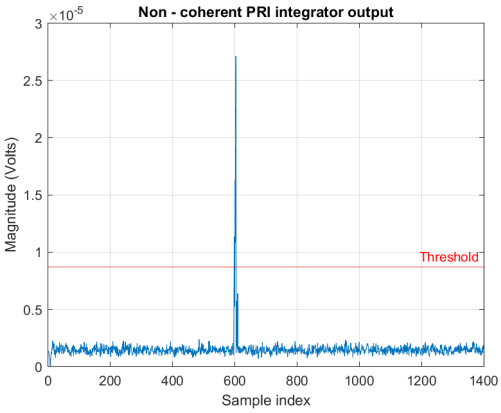

(c) Target at $120°$.

Figure 19: Signals at non-coherent PRI integrator's output.